J|A|C|S COMMUNICATIONS

Published on Web 07/22/2009

Size Control of Arsenic Trioxide Nanocrystals Grown in Nanowells

Eun-Ah You,[†] Richard W. Ahn,[†] Min Hyung Lee,[†] Meera R. Raja,[†] Thomas V. O'Halloran,*[,†,ξ] and Teri W. Odom*[,†,‡]

Department of Chemistry Department of Materials Science and Engineering, Department of Biochemistry, Molecular Biology and Cell Biology, Northwestern University, 2145 Sheridan Road, Evanston, Illinois 60208-3133

Received March 18, 2009; E-mail: t-ohalloran@northwestern.edu; todom@northwestern.edu

The development of nanotherapeutic drug delivery vehicles has revealed that size is an important factor in determining the pharmacokinetics, biodistribution, and efficacy of therapeutic agents in vivo.[1] There are numerous advantages to nanoscale therapeutics including: (1) passive targeting of nanoparticles to tumors via the enhanced permeability and retention (EPR) effect; (2) the availability of a surface for modification with stabilizing agents/targeting ligands; and (3) tunable solubility by controlling surface-to-volume ratios.[1−3] Few general methods exist, however, to control the size of nanoparticulate forms of the growing class of inorganic anticancer agents. To address this problem, we have carried out a bottom-up meets top-down approach to produce nanocrystalline drugs using the FDA-approved anticancer arsenic trioxide (ATO) as a model system.

ATO is a highly efficacious agent for acute promyelocytic leukemia and an emerging treatment for multiple myeloma.[4−6] While ATO-based regimens continue to expand treatment options in hematological cancers, the clinically achievable dose is less effective for solid tumors, in part because of efficient renal excretion of free ATO.[7,8] The development of a nanoparticle formulation of ATO, including lipid encapsulated versions that undergo pH-dependent As(III) release,[9] will likely extend the circulation half-life of ATO. This effect has been observed for other drugs reformulated as nanoparticles.[1] Although ATO particles with diameters of 40 and 80 nm have been prepared by sol−gel methods, the overall particle size was not well controlled.[10] Therefore, a more robust method is needed to control particle size to optimize drug efficacy. Here we describe a strategy for achieving size control of ATO nanocrystals over a wide range of diameters using nanowell arrays as confined reaction vessels. We tested these particles against the K562 human chronic myeloid leukemia cell line and found that ATO nanocrystals modestly attenuated activity compared to free ATO.

Crystallization in microwells via discontinuous dewetting favors single nucleation events,[11] and the rapid evaporation of solvent results in the formation of crystalline materials.[12] Our previous work demonstrated that when simple, inorganic materials (NaCl, CdS) were grown in silicon nanowells of zL-volumes, only single crystalline particles were formed. Their sizes could be controlled by changing the concentration of the precursor solution.[13] Figure 1A shows a scheme of how this general methodology can be extended to produce nanocrystalline drugs using polymer nanowell substrates. The nanowells were fabricated out of SU-8 (a negative-tone photoresist) on glass substrates in square arrays on a 2-μm pitch by exposing the photoresist to UV light through a hard PDMS (poly(dimethylsiloxane)) mask patterned with ca. 300-nm recessed cylindrical posts.[14] The volume of the fabricated nanowells was determined by (1) molding PDMS against the nanowell array so that the diameter d could be analyzed by scanning electron microscopy (SEM) and (2) measuring the height h by atomic force microscopy (AFM). Typical wells had d = 600 nm and h = 70−80 nm for a well-volume of ca. 20 aL. The nanowell diameters were larger than the features on the PDMS mask because that part of the lithography process requires a postbake (95 °C) of the SU-8, which tends to increase the sizes of the structures.

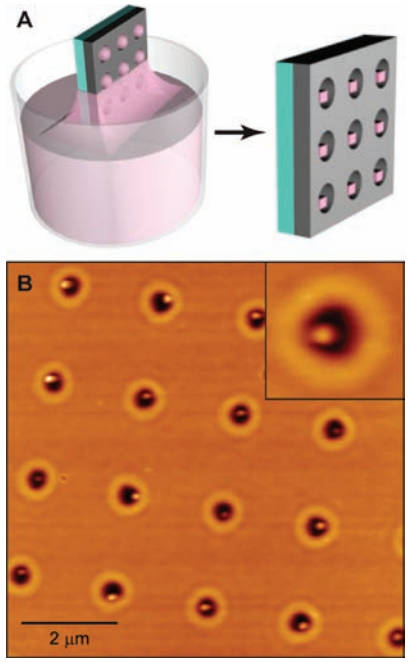

Figure 1. (A) Scheme for filling nanowells with ATO solution by discontinuous dewetting. (B) AFM image of nanowells with ATO crystals generated from a 100-mM ATO solution.

To control the sizes of ATO nanocrystals, we kept the volume of the nanowells fixed and varied the concentrations of the ATO solution. Solutions were prepared by dissolving coarse ATO powder (Sigma-Aldrich, 99.995% purity) with ultrapure water (18 MΩ); sodium hydroxide (NaOH) was added to accelerate ATO dissolution. The optimum molar ratio of NaOH to ATO for the formation of nanocrystals was determined to be 7.5:1; this ratio was maintained for all ATO solutions. Four different

[†] Department of Chemistry.
[ξ] Department of Biochemistry, Molecular Biology and Cell Biology.
[‡] Department of Materials Science and Engineering.

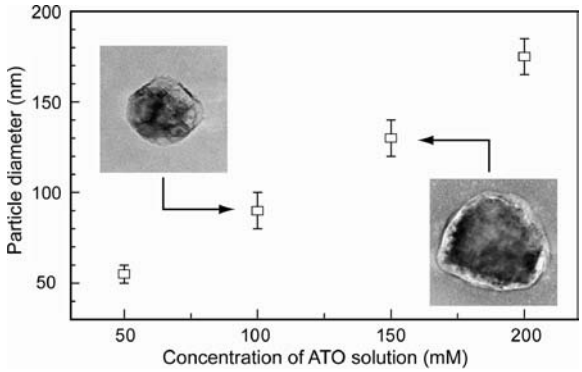

Figure 2. Sizes of ATO nanocrystals as a function of different concentrations of ATO solutions. Images are 150 nm × 150 nm.

concentrations of ATO solutions (50, 100, 150, and 200 mM) were used to grow ATO nanocrystals.

We used discontinuous dewetting to fill the nanowell arrays with ATO solution at a drawing rate of 20 μm/s using a syringe pump. ATO nanocrystals were formed in the wells after rapid evaporation of the water solvent (Figure 1B) and were released from the nanowells by sonication in water (30 s). The diameter and distribution of ATO nanocrystals were measured by transmission electron microscopy (TEM) at each ATO concentration. As anticipated,[13] higher ATO concentrations produced larger particle sizes: (1) 50 mM, 55 ± 5 nm; (2) 100 mM, 90 ± 10 nm; (3) 150 mM, 130 ± 10 nm; and (4) 200 mM, 175 ± 10 nm (Figure 2).

We compared the sizes of the ATO nanocrystals measured by TEM (d) and AFM (h) with those estimated by considering the well volume, concentration of ATO, and density of ATO (ρ = 3.86 g/cm^3).[15] The total reaction volume consisted of the well volume plus a convex meniscus of 70.4°−72.0° over the top of the well; these angles were determined by contact angle measurements of ATO solutions on the surface of SU-8. The discrepancy between calculated and measured volumes of ATO nanocrystals was less than 20% for some concentrations, with the largest error occurring at the lowest concentrations (Table S1). The average sizes and dispersity of ATO nanocrystals determined by dynamic light scattering (DLS) were in agreement with the sizes determined by TEM (Table S2).

Selected area electron diffraction (SAED) revealed that nanocrystals formed from all four ATO solutions were single crystalline. Analysis of the diffraction pattern (Figure 3A, inset) revealed a lattice spacing of 0.277 nm when viewed along the [001] axis, which corresponds to a cubic structure. The SAED patterns were consistent with the crystal structure of arsenolite As_2O_3, which has space group $Fd3m$.[16] Elemental analysis of the ATO nanocrystals by energy dispersive X-ray spectroscopy showed elemental ratios of As/O/Na to be 40:60:0(%), which indicated that the nanocrystals did not contain Na (Figure S1). The surface charge of nanoparticles is important for predicting clearance, aggregation, and surface functionalization conditions.[1] Zeta potential measurements showed that ATO nanocrystals had a small negative surface charge, approximately −20 mV, which is comparable to FDA approved agents such as DOXIL.[17]

Although the nanowell arrays in Figure 1B could produce nanocrystalline drugs with well-controlled sizes, the quantity of ATO nanocrystals per chip was not sufficient for *in vitro* studies. Hence, we developed a molding process (compared to photolithography) to fabricate nanowell substrates with higher densities. We used a variant of soft interference lithography[18] to generate PDMS nanowells on a 400-nm pitch, which resulted in nanowell densities 25 times higher than those of the SU-8 nanowells on a 2-μm pitch (Figure S2). To fabricate these high density nanowells, PDMS was molded against a polyurethane (Norland Optics, NOA 81) master patterned with an array of 230-nm circular posts. The patterned area covered ca. 26 cm^2. This molding approach is also advantageous for scaling because the PDMS nanowells can be replicated hundreds of times from a single polyurethane master. The nanowells had d = 230 nm and h = 100 nm for a well volume of ca. 4 aL. Because most nanotherapeutic work has focused on nanoparticles with diameters less than 100 nm,[2] we decided to create nanocrystals of similar sizes. Based on results from Figure 2 and Table S1 (convex meniscus with the measured contact angle of 89.0° for PDMS), we estimated that ATO nanoparticles with diameters between 50 and 100 nm should be formed from 300 mM ATO solutions. Indeed, after discontinuous dewetting, ATO nanocrystals were formed in PDMS nanowells with an average diameter of ca. 70 nm (Figure S3) and in sufficient yield to produce a 300 μM (elemental As) stock solution for bioactivity assays.

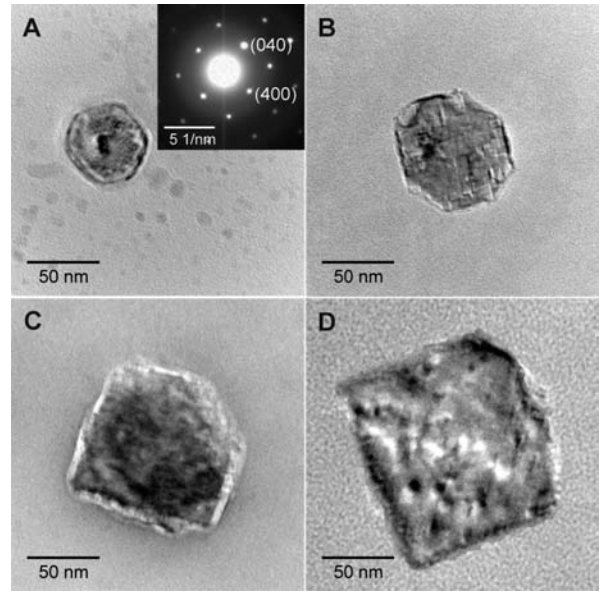

Figure 3. TEM images of ATO nanocrystals generated from (A) 50, (B) 100, (C) 150, and (D) 200 mM ATO solutions. Inset: SAED of ATO crystals.

To examine whether the nanocrystalline form retained biological activity, the cytotoxicity of 70-nm ATO nanocrystals was compared with free ATO in K562 cells, a human chronic myeloid leukemia cell line. Cells were treated with varied concentrations of either ATO nanocrystals or free ATO for 24 h, and the number of viable cells was measured using a soluble tetrazolium salt (MTS) that is converted into a colored formazin product in living cells (Supporting Information). The percentage of viable cells was plotted against the concentration of elemental As, and a sigmoidal dose−response curve was fit to the data (Figure 4). Arsenic concentrations in media were determined by inductively coupled plasma-mass spectrometry (ICP-MS) for both nanocrystalline ATO and free ATO. The concentration of As resulting in 50% growth inhibition (IC_{50}) was 5.2 μM for ATO nanocrystals and 3.8 μM for free ATO. Therefore, the ATO

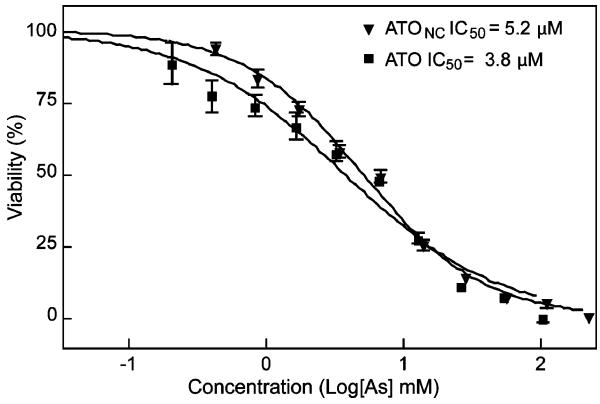

Figure 4. Cytotoxicity (IC_{50}) of ATO nanocrystals (ATO_{NC}; $IC_{50} = 5.2$ μM [95% Confidence Interval (CI) 4.8−5.7]) and free ATO ($IC_{50} = 3.8$ μM [95% CI 3.4−4.3]) against K562 human chronic myeloid leukemia cells. Error bars represent the standard error of the mean ($n = 12$ wells).

nanocrystals have a biological potency that is similar to, and slightly lower than, that of the parent drug. A slow rate of nanoparticle dissolution may account for the small difference in activity.

In summary, we demonstrated a new strategy to synthesize nanocrystalline forms of potent inorganic anticancer drugs by the evaporation of solvents from small-volume reactors. The sizes of ATO nanocrystals were controlled from 55−175 nm by simply changing the concentrations of ATO solution. *In vitro* studies suggested that the nanocrystalline formulation of ATO has cancer cell killing activity that is comparable to that of the parent drug in K562 leukemia cells. The nanocrystalline formulation of ATO likely dissolves more slowly, which could result in an extended serum half-life and allow for less frequent dosing.

These results suggest that nanocrystalline formulations of emerging anticancer agents are accessible and can be readily scaled up. Manipulation of the physical form of such agents is known to increase the efficacy of chemotherapeutics by extending the release profile of the drug. Our method constitutes a significant step forward for developing a new formulation of ATO and lays the groundwork for expanding the profile of this agent beyond hematological cancers and into solid tumors.[9,19] The development of nanocrystalline therapeutics enables the delivery of high densities of drug that can concentrate in solid tumors via the EPR effect.[20] Looking forward, the routine availability of ATO nanocrystals will enable passivation with lipids and polymers and serve as a platform for ligands and peptides to target cancer cells.[21,22] We anticipate this approach can be broadly applied to create other nanocrystalline drugs such as cisplatin and doxorubicin with well-controlled sizes.

Acknowledgment. This work was supported by the CCNE at Northwestern University (NU) (NCI U54CA119341) (TWO, TVO), CDMRP BCRP Fellowship (BC073413) (RWA), R. H. Lurie Cancer Center Malkin Scholarship (RWA), NSF CMMI-0826219, and the David and Lucile Packard Foundation. We thank the staff of the High Throughput Analysis Facility, EPIC, QBIC, NIFTI, and NUANCE at NU.

Supporting Information Available: DLS, EDS spectra, cell cytotoxicity results, ICP-MS data, and calculations of volume sizes of ATO nanocrystals. This material is available free of charge via the Internet at http://pubs.acs.org.

References

(1) Li, S. D.; Huang, L. *Mol. Pharm.* **2008**, *5*, 496–504.
(2) Davis, M. E.; Chen, Z. G.; Shin, D. M. *Nat. Rev. Drug Discovery* **2008**, *7*, 771–782.
(3) Rabinow, B. E. *Nat. Rev. Drug Discovery* **2004**, *3*, 785–796.
(4) Tallman, M. S. *Best Pract. Res. Clin. Haematol.* **2008**, *21*, 659–666.
(5) Evens, A. M.; Tallman, M. S.; Gartenhaus, R. B. *Leuk. Res.* **2004**, *28*, 891–900.
(6) Murgo, A. J. *Oncologist* **2001**, *6* (Suppl 2), 22–28.
(7) Maeda, H.; Hori, S.; Nishitoh, H.; Ichijo, H.; Ogawa, O.; Kakehi, Y.; Kakizuka, A. *Cancer Res.* **2001**, *61*, 5432–5440.
(8) Brunet, C.; Luyckx, M.; Cazin, M. *Toxicol. Eur. Res.* **1982**, *4* 175–179.
(9) Chen, H.; MacDonald, R. C.; Li, S.; Krett, N. L.; Rosen, S. T.; O'Halloran, T. V. *J. Am. Chem. Soc.* **2006**, *128*, 13348–13349.
(10) Wang, Z.; Zhang, D.; Gu, N.; Lu, X.; Yan, S. *J. Southeast Univ.* **2005**, *21*, 58–62.
(11) Jackman, R. J.; Duffy, D. C.; Ostuni, E.; Willmore, N. D.; Whitesides, G. M. *Anal. Chem.* **1998**, *70*, 2280–2287.
(12) Thalladi, V. R.; Whitesides, G. M. *J. Am. Chem. Soc.* **2002**, *124*, 3520–3521.
(13) Barton, J. E.; Odom, T. W. *Nano Lett.* **2004**, *4*, 1525–1528.
(14) Odom, T. W.; Thalladi, V. R.; Love, J. C.; Whitesides, G. M. *J. Am. Chem. Soc.* **2002**, *124*, 12112–12113.
(15) Panta, P. *Handbook of inorganic chemicals*; McGraw-Hill Professional: 2002.
(16) Ballirano, P.; Maras, A. *Z. Kristallogr. NCS* **2002**, *217*, 177–178.
(17) Garbuzenko, O.; Zalipsky, S.; Qazen, M.; Barenholz, Y. *Langmuir* **2005**, *21*, 2560–2568.
(18) Henzie, J.; Lee, M. H.; Odom, T. W. *Nature Nanotechnol.* **2007**, *2*, 549–554.
(19) Verstovsek, S.; Giles, F.; Quintas-Cardama, A.; Perez, N.; Ravandi-Kashani, F.; Beran, M.; Freireich, E.; Kantarjian, H. *Hematol. Oncol.* **2006**, *24*, 181–188.
(20) Ganta, S.; Paxton, J. W.; Baguley, B. C.; Garg, S. *Int. J. Pharm.* **2009**, *367*, 179–186.
(21) Chen, H.; Ahn, R.; Van den Bossche, J.; Thompson, D. H.; O'Halloran, T. V. Mol. Cancer Ther. 2009 (Online First June 30, 2009).
(22) Lee, S.-M.; Chen, H.; O'Halloran, T. V.; Nguyen, S. T. *J. Am. Chem. Soc.* **2009**, *131*, 9311–9320.

JA902117B